Silicon recovery from silicon-iron alloys by electrorefining in molten fluorides

Laurent Massot, Anne-Laure Bieber, Mathieu Gibilaro, Laurent Cassayre, Pierre Taxil, Pierre Chamelot

▶ **To cite this version:**

Laurent Massot, Anne-Laure Bieber, Mathieu Gibilaro, Laurent Cassayre, Pierre Taxil, et al.. Silicon recovery from silicon-iron alloys by electrorefining in molten fluorides. Electrochimica Acta, 2013, vol. 96, pp. 97-102. 10.1016/j.electacta.2013.02.065 . hal-00805734

HAL Id: hal-00805734
https://hal.science/hal-00805734

Submitted on 28 Mar 2013

HAL is a multi-disciplinary open access archive for the deposit and dissemination of scientific research documents, whether they are published or not. The documents may come from teaching and research institutions in France or abroad, or from public or private research centers.

L'archive ouverte pluridisciplinaire **HAL**, est destinée au dépôt et à la diffusion de documents scientifiques de niveau recherche, publiés ou non, émanant des établissements d'enseignement et de recherche français ou étrangers, des laboratoires publics ou privés.

Open Archive TOULOUSE Archive Ouverte (OATAO)

OATAO is an open access repository that collects the work of Toulouse researchers and makes it freely available over the web where possible.

This is an author-deposited version published in : http://oatao.univ-toulouse.fr/
Eprints ID : 8620

To link to this article : DOI: 10. 1016/j.electacta.2013.02.065
URL : http://dx.doi.org/10.1016/j.electacta.2013.02.065

To cite this version : Massot, Laurent and Bieber, Anne-laure and Gibilaro, Mathieu and Cassayre, Laurent and Taxil, Pierre and Chamelot, Pierre *Silicon recovery from silicon-iron alloys by electrorefining in molten fluorides.* (2013) Electrochimica Acta, vol. 96 . pp. 97-102. ISSN 0013-4686

Any correspondence concerning this service should be sent to the repository administrator: staff-oatao@listes.diff.inp-toulouse.fr

Silicon recovery from silicon–iron alloys by electrorefining in molten fluorides

L. Massot*, A.L. Bieber, M. Gibilaro, L. Cassayre, P. Taxil, P. Chamelot

Université de Toulouse; UPS, INP, CNRS; Laboratoire de Génie Chimique; Département Procédés Electrochimiques; 118 Route de Narbonne, 31062 Toulouse, France

A B S T R A C T

Electrorefining of a silicon-iron material (Si–4.7 at% Fe) in molten NaF-KF at 850 °C was investigated in view of recovering pure Si, using electrochemical techniques, Scanning Electron Microscopy coupled with Energy Dispersive Spectroscopy (SEM-EDS) and Inductively Coupled Plasma with atomic emission spectroscopy (ICP-AES) analyses. The selective electrochemical dissolution of Si was evidenced. Electrorefining runs led to a maximum recovery of 80% of Si initially contained in the material, in the form of a dense deposit at the cathode, with very high current efficiencies. The Si purity was examined and no Fe was detected by ICP-AES analysis: the recovered Si purity was assumed to be higher than 99.99%.

Keywords:
Molten fluorides
Silicon
Electrorefining
Si–Fe alloys
Voltammetry

1. Introduction

Photovoltaic technology is a very important renewable source of electrical energy production with the highest annual growth rate [1,2] and the most common base material for photovoltaic cell is Solar Grade Silicon (SoG-Si), with a required purity of 99.9999%. Due to a growing demand for SoG-Si, the development of new processes allowing the production of cheaper SoG-Si is a main issue for the solar energy industry [3]. In the 1980's, silicon electrodeposition in molten salts has been considered as an attractive option for SoG-Si production [4]. However, the electrolytic Si production process has not found any commercial application up to now. In the frame of more recent concerns about carbon-free energy production, such kind of process has nevertheless been reassessed. Thus, basic investigations on Si(IV) reduction mechanism have been carried out in molten fluorides [5–14] and more recently, the salts properties and silicon deposition strategies were examined in our laboratory [15,16]. These results concluded that Si(IV) ions are reduced into Si in a one-step process exchanging four electrons controlled by diffusion in the solution.

The final objective of the study is to evaluate the feasibility of using electrorefining process in molten fluorides as preliminary step of purification of metallurgical grade Si (MG-Si) with good quality.

Table 1 compares the composition of MG-Si and the maximum admissible impurity content in SoG-Si. These data show first that oxygen and iron are the most important pollutants of MG-Si and then, that the highest tolerance in SoG-Si is for carbon, oxygen and iron [17–19]. In this work, only metallic impurities (M_i) were taken into account. More specifically, the present work is focused on the separation of silicon and iron by electrolysis at laboratory scale, in a molten fluoride mixture, through the dissolution of a Si–Fe anode, with the operating conditions defined in references [15,16]. The study was divided into three parts: (i) determination of the Si–Fe dissolution pathway by electrochemical techniques coupled with SEM observations and EDS analysis, (ii) silicon deposits purity examination with EDS and ICP-AES analyses and (iii) anodic and cathodic current efficiencies evaluation by weighting the electrodes.

2. Experimental

2.1. Cell

The cell was a vitreous carbon crucible placed in a cylindrical vessel made of refractory steel and closed by a stainless steel lid cooled by circulating water. The description of this cell has been detailed in previous work [20]. The experiments were performed under an inert argon atmosphere (Linde). The cell was heated using a programmable furnace and the temperature was measured using a chromel-alumel thermocouple. The electrolytic bath consisted of the NaF-KF (40–60 mol%) eutectic mixture (Carlo Erba 99.99%). The mixture was initially dehydrated by heating under vacuum (6×10^{-2} mbar) from ambient temperature up to its melting point during one week. Silicon solute was introduced into the bath in

* Corresponding author. Tel.: +33 561558194; fax: +33 561556139.
E-mail address: massot@chimie.ups-tlse.fr (L. Massot).

Table 1
Comparison between impurities content in MG-Si and maximum admissible content (ppm) in SoG-Si.

Impurities	MG-Si	SoG-Si (Maximum content)
B	20–50	<1
P	25–50	<1
O	3000	<10
C	10–250	<10
Fe	1000–3000	<10
Al, Ca	100–1500	<2
Other metals (Ti, Cr, Mn, Ni, Cu, Zr. . .)	5–150	<1

the form of sodium hexafluorosilicate Na_2SiF_6 (Alfa Aesar 99.99%) powder.

2.2. Electrodes

Iron, copper, nickel, titanium, silicon plate (4 mm × 8 mm × 11 mm) (Goodfellow 99.99%), molybdenum (Goodfellow 99.95%), chromium, manganese and zirconium (Goodfellow 99.5%) wires (1 mm diameter) and 95.3 at% Si–4.7 at% Fe alloy (8 mm diameter) were used as electrodes. The surface area of the working electrode was determined after each experiment by measuring the immersion depth in the bath. The auxiliary electrodes were silicon plate (4 mm × 8 mm × 11 mm) and graphite carbon rods (3 mm diameter – Mersen spectroscopic quality) with a large surface area (3 cm^2). A platinum wire immersed in the molten electrolyte was used as a quasi-reference electrode.

2.3. Techniques

The electrochemical technique used for the anodic behaviour investigation of each material was linear voltammetry, at a scan rate of 10 mV s^{-1}, while electrorefining runs were carried out by imposition of a constant cathodic current. All the electrochemical polarizations were performed with an Autolab PGSTAT 30 potentiostat/galvanostat controlled by a computer using the research software GPES 4.9.

The electrodes surface and cross-section were characterized by Scanning Electron Microscope (SEM) coupled with Energy Dispersive Spectroscopy (EDS) probe, after residual salt removal in $HCl–AlCl_3–H_2O$ mixture at 50 °C and ultrasonic waves.

Si and Fe content of both salt and deposit samples were measured, after dissolution, using Inductively Coupled Plasma-Atomic Emission Spectroscopy (ICP-AES, HORIBA Ultima 2).

3. Results and discussion

3.1. Operating conditions for silicon electrorefining

Electrorefining is a method applied for purifying metals using an electrolysis cell. It consists in an anodic dissolution of the material to be purified and a deposition of the target metal without impurities on the cathode. Three main issues have to be considered: the anodic behaviour of the material, the stability of the dissolved species in the molten salt and the electrodeposition conditions at the cathode. In the specific case of Si electrorefining, two steps (Si(IV) stability in the salt and Si deposition) have already been investigated in our laboratory [15,16], as detailed below, while the Si selective dissolution remains to be demonstrated.

Concerning the Si(IV) stability, it has been shown that in molten fluoride salts, Si(IV) ions are solvated as SiF_{4+x}^{x-} in equilibrium with gaseous SiF_4, according to the equilibrium (1).

$$SiF_{4+x}^{x-} = SiF_{4(g)} + xF^- \quad (1)$$

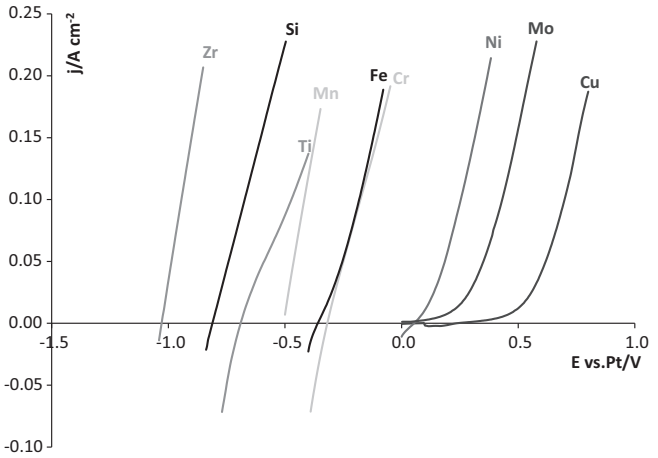

Fig. 1. Comparison of linear voltammograms (anodic part) on various metals at 10 mV s^{-1} in NaF-KF at 850 °C; Aux. El.: vitreous carbon; Ref El.: Pt.

Bieber et al. shows that SiF_{4+x}^{x-} stability is highly influenced by the fluoroacidity (free F^- ions content) and that SiF_{4+x}^{x-} is more stable in basic molten baths: the most suitable one was proven to be the eutectic NaF-KF (40–60 mol%) mixture [15]. In order to minimize Si losses in the gaseous phase, this salt mixture ($T_{melting}$ = 718 °C) has thus been selected for the electrorefining runs.

It has been stated that the electrochemical reduction of Si(IV) ions is a one-step process exchanging 4 electrons, whatever the fluoride salt composition, as indicated in reaction (2).

$$Si(IV) + 4e^- = Si \quad (2)$$

A detailed nucleation and electrodeposition study has been performed [16] and led to the following conclusions:

- an operating temperature of 850 °C, about 130 °C above the solvent melting point, allows to enhance Si electrical conductivity,
- graphite or SoG-Si cathodic substrates ensure the best adherence to Si deposits,
- a Si(IV) concentration higher than 0.6 mol kg^{-1} inhibits potassium insertion into the deposit at a cathodic current density of −50 mA cm^{-2}.

These experimental conditions have thus been applied to the Si electrorefining in molten fluorides.

3.2. Impact of impurities on the electrorefining selectivity

3.2.1. Preliminary discussion

The selectivity of the electrorefining process depends on the dissolution potentials (E_{diss}) of the metals to be treated. In the frame of electrorefining of Si base materials containing an impurity M_i, three cases have to be considered:

- case 1: $E_{diss}^{Mi} > E_{diss}^{Si}$. The impurity is not dissolved during anodic dissolution of Si: the selectivity of the process is thus governed by the anode potential.
- case 2: $E_{diss}^{Mi} < E_{diss}^{Si}$. The impurity is dissolved together with Si but is not reduced at the cathode due to a lower reduction potential: the selectivity of the process is ensured by the control of the cathode potential.
- case 3: $E_{diss}^{Mi} \sim E_{diss}^{Si}$. The impurity is dissolved together with Si: complete electrochemical reduction behaviour has to be studied in order to evaluate the possibility of its co-deposition with silicon. In this last case, the separation is expected to be difficult.

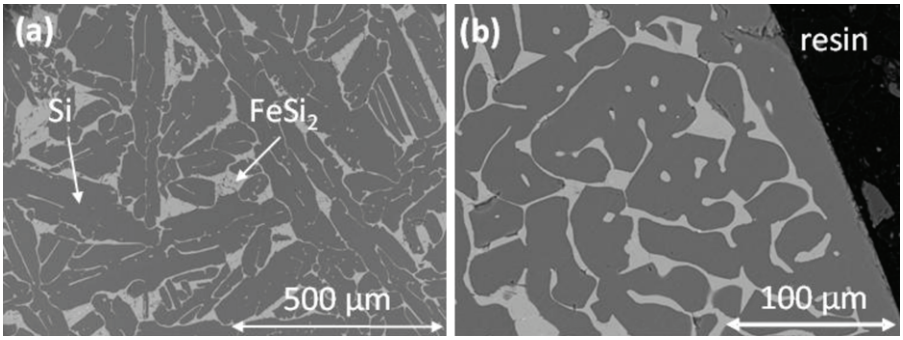

Fig. 2. SEM micrographs of the cross section of the Si–4.7 at% Fe anode: (a) bulk; (b) external surface (light grey: $FeSi_2$; dark grey: Si).

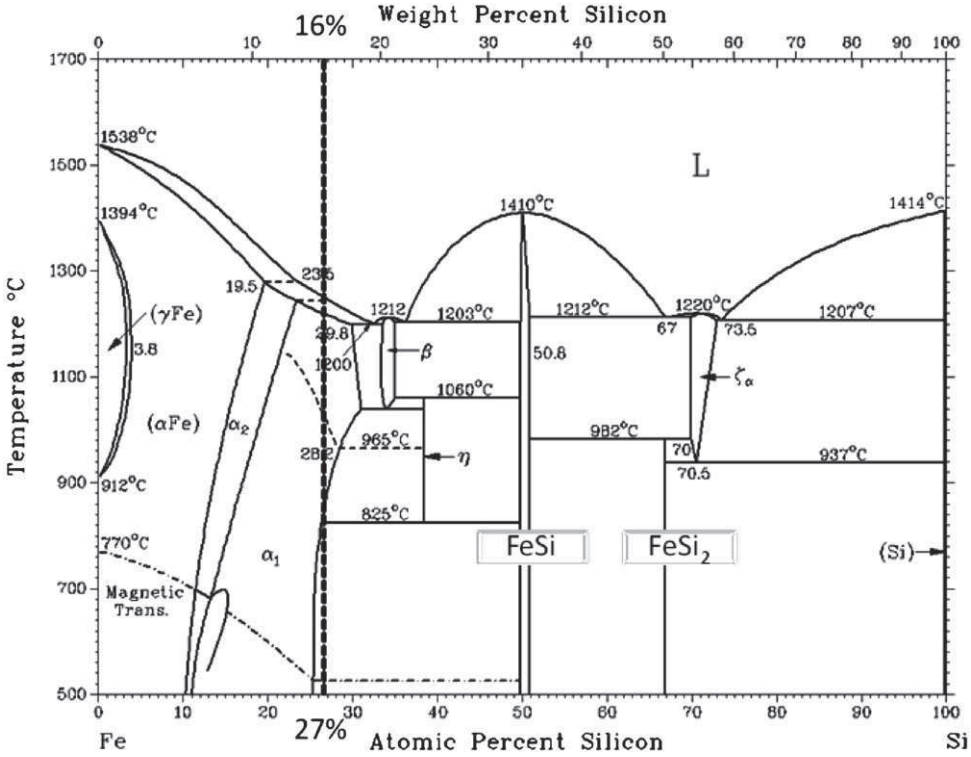

Fig. 3. Fe–Si phase diagram [9].

The electrochemical behaviour of several metals considered as common pollutant in SoG-Si has been studied by linear sweep voltammetry in NaF-KF at 850 °C. Linear voltammograms recorded at 10 Mv s^{-1} are plotted in Fig. 1.

The three cases previously mentioned are highlighted in this figure: Cu, Mo, Ni, Cr and Fe correspond to case 1, Zr to case 2, Ti and Mn to case 3.

Iron (case 1) was selected as a "model impurity" due to its relatively close oxidation potential compared to Si ($\Delta E \sim 450$ mV). In order to demonstrate the feasibility of Si–Fe separation and to evaluate current efficiencies, a commercial Si–4.7 at% Fe alloy with a rather high Fe content was used.

3.2.2. Characterization of the Si–4.7 at%Fe anode

The microstructure of the anode material, as illustrated in Fig. 2 by SEM micrographs of its cross-section, is composed of two phases: a silicon matrix and an intermetallic compound, $FeSi_2$, in agreement with the Si–Fe phase diagram (Fig. 3) [21]. Based on available density data (ρ(Si) = 2.3 g mL^{-1} and $\rho(FeSi_2)$ = 4.7 g mL^{-1} [22]), the volume of the intermetallic phase within the matrix is about 11%.

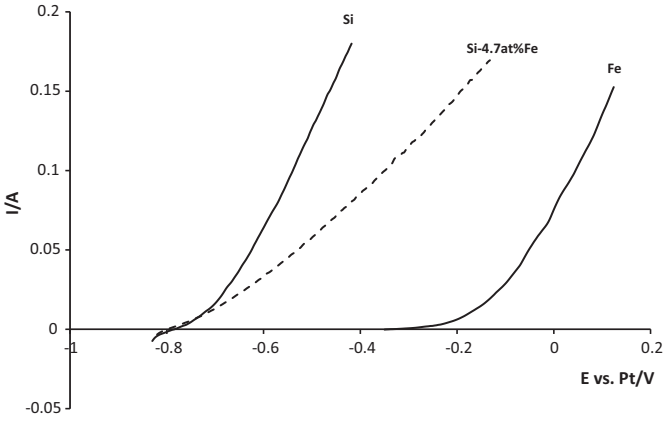

Fig. 4. Comparison of linear voltammograms of Si, Fe and Si–4.7 at% Fe at 10 mV s^{-1} in NaF-KF at 850 °C; Aux. El.: vitreous carbon; Ref. El.: Pt.

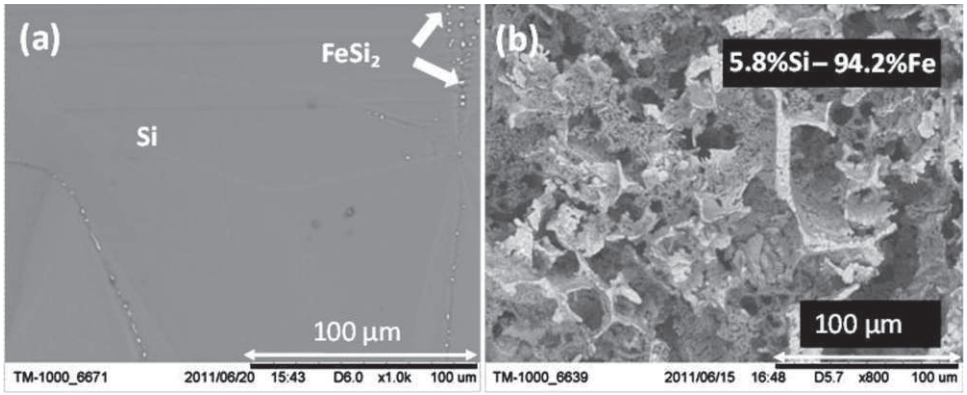

Fig. 5. SEM micrographs of the Si–4.7 at% Fe anode surface: (a) before electrolysis and (b) after electrolysis in NaF-KF-Na_2SiF_6 (C = 0.73 mol kg^{-1}) during 25 h at 50 mA cm^{-2} at 850 °C (Q = 8659 C).

Fig. 4 exhibits the anodic behaviour of Si, Fe and Si–4.7 at% Fe recorded by linear sweep voltammetry in the NaF-KF system at 850 °C and 10 mV s^{-1}. This figure verifies that the dissolution of Fe occurs at a more positive potential than Si. Concerning the Si–Fe alloy, the shape of the linear voltammogram could be explained by the two-phase structure of the anode: Si and $FeSi_2$. As observed in Fig. 2, the sample is composed of pure Si matrix with $FeSi_2$ phase. As the Si oxidation potential is lower than Fe and according to Nernst law, only the pure Si phase is first oxidized, explaining why the equilibrium potential is the same than Si sample. Then, after short polarization duration, Si is oxidized from both pure Si and $FeSi_2$ phases; and according to Nernst law for Si activity lower than 1, the Si oxidation rate is lowered.

3.3. Si electrorefining process

The optimized experimental conditions for Si electrorefining, reminded in Section 3.1, have been applied to the Si–4.7 at% Fe alloy.

3.3.1. Si–Fe anode dissolution pathway

The selective anodic dissolution was demonstrated first. Electrolysis runs were performed in NaF-KF-Na_2SiF_6 (0.73 mol kg^{-1}) system, at 850 °C and a current density of 50 mA cm^{-2} during 25 h, and Fig. 5 shows SEM micrographs of the Si–Fe anode surface before (a) and after (b) electrolysis. Before electrolysis, both Si and $FeSi_2$ phases are observed whereas, after electrolysis, the residual structure has a "sponge-like" shape and is composed of around 94.2 at% of Fe.

Magnifications of the anode cross sections are presented in Fig. 6, for short (5 h) and longer (25 h) electrolysis durations. They indicate the selective dissolution of silicon: for short duration (Fig. 6a), the pure silicon phase is removed while the $FeSi_2$ phase is depleted in Si at the anode-bath interface, forming FeSi and a phase containing 27.5 at% of Si. For longer electrolysis (Fig. 6b), the silicon matrix is more deeply dissolved (~600 µm), while Si–Fe phases remain in this area.

The composition profile of the anode after an electrorefining run of 25 h was investigated (see Fig. 7). This profile evidences the decrease of the Si content in intermetallic phases from 66.5 to 27.5 at%, from the core to the electrode surface, exhibiting the following dissolution behaviour:

- the pure Si phase was dissolved up to 600 µm.
- Si in the $FeSi_2$ phase was selectively removed to the residual value of 5.8 at%, through the formation of Fe-rich compounds previously mentioned: FeSi and Fe–27.5 at% Si, in agreement with the dissolution of a solid solution [23].

3.3.2. Si deposits purity

Fig. 8 shows silicon coatings obtained after electrorefining experiments on two cathodes: SoG-Si (a) and graphite (b), after residual salt removal. The Si deposits were adherent and their roughness was relatively high.

EDS analysis indicates that the purity of silicon deposit is higher than 99.9%, corresponding to the detection limit of the apparatus for elements titration (see EDS spectrum of Fig. 9). For more accurate quantification of Fe, the Si coating was dissolved into KOH 15 mol L^{-1} and Fe was analysed by ICP-AES in this solution: no Fe was significantly detected, meaning that the Fe concentration is less than the detection limit which is around 10 µg L^{-1}. The Si purity is then better than 99.99%. Iron concentration in the salt was

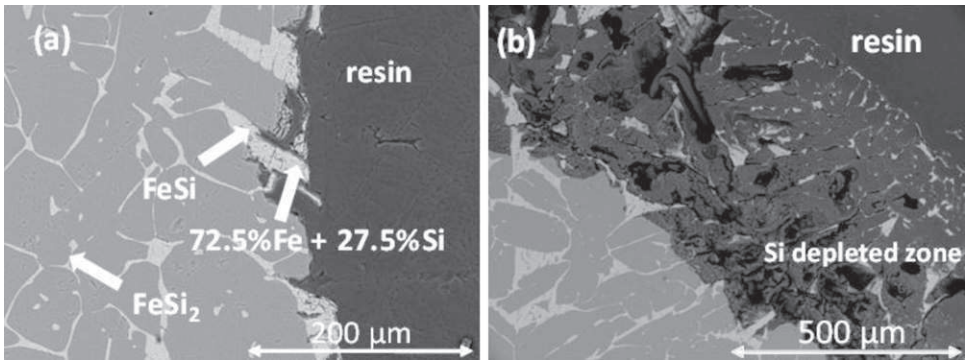

Fig. 6. SEM micrographs of the Si–4.7 at% Fe anode cross section after electrolysis in NaF-KF-Na_2SiF_6 (C = 0.73 mol kg^{-1}) at 50 mA cm^{-2} and 850 °C: (a) duration: 5 h (Q = 2448 C) and (b) duration: 25 h (Q = 8659 C).

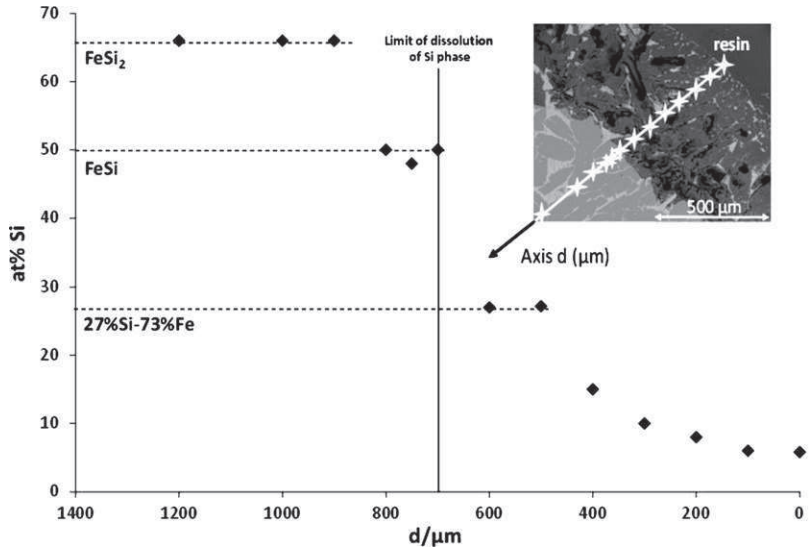

Fig. 7. Concentration profile of Si in the Si–Fe intermetallic phase after electrolysis in NaF-KF-Na_2SiF_6 ($C = 0.73$ mol kg^{-1}) at 50 mA cm^{-2} and 850 °C; duration 25 h; inset: SEM observation of the anode after electrolysis showing the location of Si analysis.

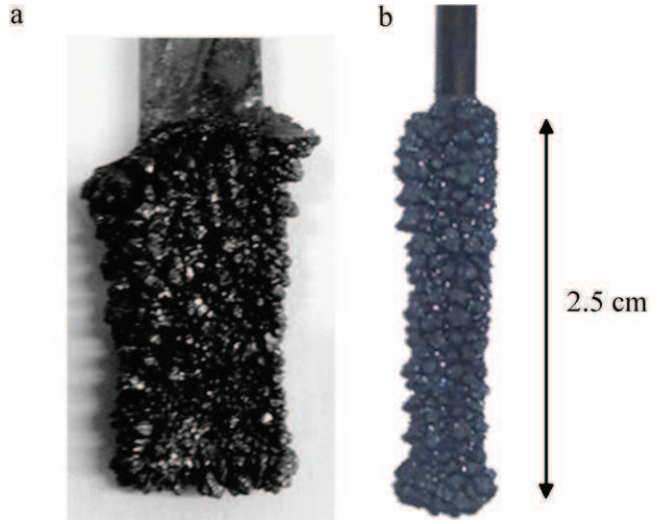

Fig. 8. Photographs of cathodes after electrolysis runs in NaF-KF-Na_2SiF_6 ($C = 0.73$ mol kg^{-1}) at 50 mA cm^{-2} at 850 °C: (a) SoG-Si cathode after 39 h; (b) graphite cathode after 25 h.

also titrated after the electrolysis and was not detected, proving that the Si dissolution is selective.

3.3.3. Current efficiencies

Anodic and cathodic current efficiencies, anodic dissolution and Si recovery progresses were estimated by comparing the final Si mass of anode and cathode to the initial mass of Si in Si–4.7 at% Fe anodes. These values were calculated according to:

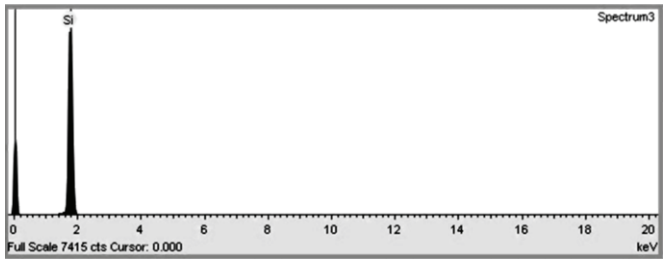

Fig. 9. EDS analysis of cathodes after electrolysis runs in NaF-KF-Na_2SiF_6 ($C = 0.73$ mol kg^{-1}) at 50 mA cm^{-2} at 850 °C: (a) SoG-Si cathode after 39 h; (b) graphite cathode after 25 h.

$$\text{Anodic dissolution progress} = \frac{\Delta m_{\text{dissolved}}}{m_{\text{Si into Si–Fe anode}}} \quad (3)$$

$\Delta m_{\text{dissolved}}$ (g) is the mass of dissolved Si evaluated from the mass balance of the anode, and $m_{\text{Si into Si–Fe anode}}$ (g) is the mass of silicon initially present in the anode. This mass was calculated by measuring the initial anode mass and correcting it by the Si composition (90 wt% Si).

$$\text{Si recovery progress} = \frac{m_{\text{Si deposited}}}{m_{\text{Si into Si–Fe anode}}} \quad (4)$$

$m_{\text{Si deposited}}$ is the silicon mass deposited.

Table 2 gathers the values obtained in several electrorefining runs, leading to the following conclusions:

Table 2
Anodic Si dissolution and cathodic Si recovery progresses and anodic and cathodic faradic efficiencies of electrorefining runs performed in NaF-KF-Na_2SiF_6 ($C = 0.73$ mol kg^{-1}) at 50 mA cm^{-2} and 850 °C.

	Q (C)	Anode: Si initial mass (g)	Anode dissolved mass (g)	Dissolution progress	Anodic faradic efficiency	Cathode: Si deposited mass (g)	Si recovery progress	Cathodic faradic efficiency
1	2448	1.851	0.178	10%	89%	0.205	11%	100%
2	5480	1.028	0.360	35%	98%	0.399	39%	92%
3	8659	1.095	0.548	50%	90%	0.648	59%	90%
4	10,391	1.076	0.646	60%	90%	0.716	67%	94%
5	13,622	1.111	0.878	79%	94%	0.989	89%	99%
6	22,248	1.755	1.457	83%	–	1.619	92%	100%
7	23,425	1.818	1.636	90%	–	1.809	99%	100%

- the faradic efficiencies are close to 100% and the difference to unity is likely attributed to material loss during frozen salt removal from electrodes,
- for experiments 6 and 7, the anode felt into the bath before the end of the run. This indicates that the limit of dissolution progress is around 80%, due to the anode structure (11 vol% Fe). At higher dissolution rate, the anodes become too brittle to ensure cohesive structure,
- the cathodic efficiency (Si recovery) reaches 99%.

4. Conclusion

This work demonstrated that electrorefining in a basic molten fluoride solvent is an option to be considered for pure silicon recovery from silicon materials containing Fe.

Previous studies stated on the best operating conditions for electrodeposition of Si: solvent (eutectic NaF-KF), temperature (850 °C), Si(IV) concentration (>0.6 mol kg^{-1}) and current density (50 mA cm^{-2}).

Electrorefining runs evidenced that electrodissolution of Si from a Si–Fe anode involved a selective release of Si within the electrolyte, a remaining Fe rich "skeleton" structure and a complete recovery of pure silicon at the cathode. It is likely that, in the case of materials with lower initial Fe contents, the remaining Fe rich phase will not form a solid structure but rather fall off and sediment in the bottom of the cell.

Moreover, the anodic and cathodic current efficiencies are close to 100% and the Si deposits purity is assumed to be higher than 99.99%, as no Fe was detected by ICP-AES analysis of the deposit.

The electrorefining method, demonstrated in this work in the specific case of Fe, is most probably suited for the purification of Si materials containing Ti, Mn, Cr, Ni, Mo and Cu since it was shown that in the NaF-KF mixture their dissolution potential is more anodic than Fe.

References

[1] M.A. Green, Recent developments in photovoltaics, Solar Energy Materials and Solar Cells 76 (2004) 3.
[2] A. Müllera, M. Ghosha, R. Sonnenscheinb, P. Woditscha, Silicon for photovoltaic applications, Materials Science and Engineering: B 134 (2006) 257.
[3] S. Pizzini, Towards solar grade silicon: challenges and benefits for low cost photovoltaics, Solar Energy Materials and Solar Cells 94 (2010) 1528.
[4] D. Elwell, R.S. Feigelson, Electrodeposition of solar silicon, Solar Energy Materials and Solar Cells 6 (1982) 123.
[5] K.H. Stern, S.M. McCollum, Electrodeposition of refractory metals from molten salts, Thin Solid Films 124 (1985) 129.
[6] U. Cohen, R.A. Huggins, Silicon epitaxial growth by electrodeposition from molten fluorides, Journal of the Electrochemical Society 123 (1976) 381.
[7] G.M. Rao, D. Elwell, R.S. Feigelson, Electrowinning of silicon from K_2SiF_6 – molten fluoride systems, Journal of the Electrochemical Society 127 (1980) 1940.
[8] G.M. Rao, D. Elwell, R.S. Feigelson, Electrodeposition of silicon onto graphite, Journal of the Electrochemical Society 128 (1981) 1708.
[9] I.G. Sharma, T.K. Mukherjee, A study on purification of metallurgical grade silicon by molten salt electrorefining, Metallurgical Transactions B 17B (1986) 395.
[10] J. De Lepinay, J. Bouteillon, S. Traore, D. Renaud, M.J. Barbier, Electroplating silicon and titanium in molten fluoride media, Journal of Applied Electrochemistry 17 (1987) 294.
[11] D. Elwell, G.M. Rao, Mechanism of electrodeposition of silicon from K_2SiF_6-flinak, Electrochimica Acta 27 (1982) 673.
[12] K.L. Carleton, J.M. Olson, A. Kibbler, Electrochemical nucleation and growth of silicon in molten fluorides, Journal of the Electrochemical Society 130 (1983) 782.
[13] D. Elwell, Electrowinning of silicon from solutions of silica in alkali metal fluoride/alkaline earth fluoride eutectics, Solar Energy Materials and Solar Cells 5 (1981) 205.
[14] R. Boen, J. Bouteillon, The electrodeposition of silicon in fluoride melts, Journal of Applied Electrochemistry 13 (1983) 277.
[15] A.L. Bieber, L. Massot, M. Gibilaro, L. Cassayre, P. Chamelot, P. Taxil, Fluoroacidity evaluation in molten salts, Electrochimica Acta 56 (2011) 5022.
[16] A.L. Bieber, L. Massot, M. Gibilaro, L. Cassayre, P. Chamelot, P. Taxil, Silicon electrodeposition in molten fluorides, Electrochimica Acta 62 (2012) 282.
[17] J.R. Davis, A. Rohatgi, R.H. Hopkins, P.D. Blais, P. Rai-Choudhury, J.R. Mccormick, H.C. Mollenkopf, Impurities in silicon solar cells, IEEE Transactions on Electron Devices 27 (1980) 677.
[18] A. Luque, S. Hegedus, Handbook of Photovoltaic Science and Engineering, J. Wiley and Sons Ltd ed., Chichester, 2003, Chap. V.
[19] F. Schmid, D.B. Joyce, Recent advances in upgrading metallurgical grade silicon for solar grade silicon feedstock, in: Proceeding of 24th EU PVSEC, Hamburg, German, 2009.
[20] L. Massot, P. Chamelot, P. Taxil, Cathodic behaviour of samarium(III) in LiF–CaF_2 media on molybdenum and nickel electrodes, Electrochimica Acta 50 (2005) 5510.
[21] O. Kubaschewski, Iron-Binary Phase Diagrams, Springer-Verlag, New York, 1982.
[22] FACT Pure substance database, http://www.factsage.com/
[23] L. Cassayre, P. Chamelot, L. Arurault, L. Massot, P. Palau, P. Taxil, Electrochemical oxidation of binary copper–nickel alloys in cryolite melts, Corrosion Science 49 (2007) 3610.